Article

Electronic Properties of Mononuclear, Dinuclear, and Polynuclear Cobaltacarboranes: Electrochemical and Spectroelectrochemical Studies

Fabrizia Fabrizi de Biani, Maddalena Corsini, Piero Zanello,
Haijun Yao, Martin E. Bluhm, and Russell N. Grimes

J. Am. Chem. Soc., **2004**, 126 (36), 11360-11369• DOI: 10.1021/ja047966l • Publication Date (Web): 20 August 2004

J|A|C|S
ARTICLES
Published on Web 08/20/2004

Electronic Properties of Mononuclear, Dinuclear, and Polynuclear Cobaltacarboranes: Electrochemical and Spectroelectrochemical Studies

Fabrizia Fabrizi de Biani,[†] Maddalena Corsini,[†] Piero Zanello,*[,†] Haijun Yao,[‡,§] Martin E. Bluhm,[‡,||] and Russell N. Grimes*[,‡]

Contribution from the Dipartimento di Chimica, Università di Siena, Via A. Moro, 53100 Siena, Italy and Department of Chemistry, University of Virginia, Charlottesville, Virginia, 22901

Received April 8, 2004; E-mail: rng@virginia.edu

Abstract: Electronic interactions and metal−metal communication in a wide range of cobaltacarborane−hydrocarbon complexes containing one to six metal centers, and exhibiting a variety of modes of intercage connectivity and molecular architectures, have been investigated via cyclic voltammetry, controlled potential coulometry, and UV−visible spectroelectrochemistry. The properties of mixed-valent Co^{III}/Co^{IV} and Co^{II}/Co^{III} species that are generated on oxidation or reduction of dinuclear and polynuclear Co^{III} complexes were examined and classified as Robin-Day Class I (localized), Class II (partially delocalized), or Class III (fully delocalized) systems. The extent of metal−metal communication between metallacarborane cage units is strongly influenced by the type of intercage connection (e.g., cage B−B or Cp−Cp); the vertexes involved (equatorial vs apical); the nature of the linking unit, if any; and the presence of substituents on the carborane cages. In multi-tripledecker complexes where three $CpCo(C_2B_3H_4)CoCp$ units are linked through a central triethynyl benzene connector, the data suggest that Co−Co electronic communication is extensive (Class III) within individual sandwich units while intersandwich delocalization is weak or absent. An extended Hückel study of $CpCoC_2B_4H_6$ double-decker and $CpCo(C_2B_3H_5)CoCp$ triple-decker sandwich model complexes shows significant differences in the orbital contributions involved in the HOMO and LUMO of the former vs the latter type. The calculations afford additional insight into the electronic structures and properties of these systems as elucidated by the experimental studies.

Introduction

Metallacarboranes of the transition elements, owing to their generally robust character, high solubility in organic solvents, and ability in many cases to undergo reversible oxidation and reduction, afford special opportunities for investigating the electronic properties of well-defined organometallic systems. In recent papers, we have elucidated the redox behavior of several families of cobaltacarborane[1,2] and ferracarborane[3a] sandwich complexes, building on earlier electrochemical investigations of small metallacarboranes.[3b] Many of these are polynuclear assemblies, where the separation between sequential oxidations or reductions allowed us to draw qualitative conclusions about the degree of intramolecular electronic delocalization in the mixed-valent species, i.e., to relate the observed K_{com} values[4] to their respective Robin-Day classifications.[5] Here, we extend our electrochemical studies to a wider series of polycobaltacarboranes having different molecular architectures, in which the building block subunits are double-decker sandwiches (Charts 1 and 2)[1,2a,6] or triple-decker assemblies (Chart 3).[1,6c,7] Our main objective in this work was to better define the nature of the mixed-valent species by comparing their preliminary classifications based on the pertinent K_{com} values (a parameter which contains different contributions, not all of which arise from mutual electronic interactions between redox centers)[1,4] with those from more selective spectroelectrochemical findings, in both cases supported by qualitative theoretical calculations.

Electrochemistry. Dinuclear Cobaltacarboranes. Compounds **3a**−**c**, **4**, **5**, **6a**−**b**, and **7a**−**b**, with their varying modes

[†] Dipartimento di Chimica, Università di Siena.
[‡] Department of Chemistry, University of Virginia.
[§] Current address: Department of Chemistry, University of Illinois, Urbana, IL 61801.
[||] Current address: Institute for Technical Chemistry (ITC−CPV), Forschungszentrum Karlsruhe, P. O.Box 3640, 76021 Karlsruhe, Germany.

(1) Yao, H.; Sabat, M.; Grimes, R. N.; Zanello, P.; Fabrizi de Biani, F. *Organometallics* **2003**, *22*, 2581.
(2) (a) Yao, H.; Sabat, M.; Grimes, R. N.; Fabrizi de Biani, F.; Zanello, P. *Angew. Chem., Int. Ed.* **2003**, *42*, 1002. (b) Yao, H.; Grimes, R. N.; Corsini, M.; Zanello, P. *Organometallics* **2003**, *22*, 4381.
(3) (a) Fabrizi de Biani, F.; Fontani, M.; Ruiz, E.; Zanello, P.; Russell, J. M.; Grimes, R. N. *Organometallics* **2002**, *21*, 4129. (b) For a listing of previous electrochemical papers in this area, see ref 3a, refs 4−7.
(4) P. Zanello, *Inorganic Electrochemistry. Theory, Practice and Application*, RS•C, Oxford, UK, United Kingdom, 2003.
(5) Robin, M. B.; Day, P. *Adv.Inorg.Chem.Radiochem.* **1967**, *10*, 247.
(6) (a) Davis, J. H., Jr.; Sinn, E.; Grimes, R. N. *J. Am. Chem. Soc.* **1989**, *111*, 4776. (b) Davis, J. H., Jr.; Sinn, E.; Grimes, R. N. *J. Am. Chem. Soc.* **1989**, 111, 4784. (c) Yao, H.; Grimes R. N. *Organometallics* **2003**, *22*, 4539. (d) Wang, X.; Sabat, M.; Grimes, R. N. *Organometallics* **1995**, *14*, 4668. (e) Curtis, M. A.; Müller, T.; Beez, V.; Pritzkow, H.; Siebert, W.; Grimes, R. N. *Inorg. Chem.* **1997**, *36*, 3602. (f) Bluhm, M.; Pritzkow, H.; Siebert, W.; Grimes, R. N. *Angew. Chem., Int. Ed.* **2000**, *39*, 4562. (g) Yao, H.; Grimes R. N. *J. Organomet. Chem.*, **2003**, *680*, 51.
(7) Yao, H.; Sabat, M.; Grimes, R. N. *Organometallics* **2002**, *21*, 2833.

10.1021/ja047966l CCC: $27.50

Chart 1

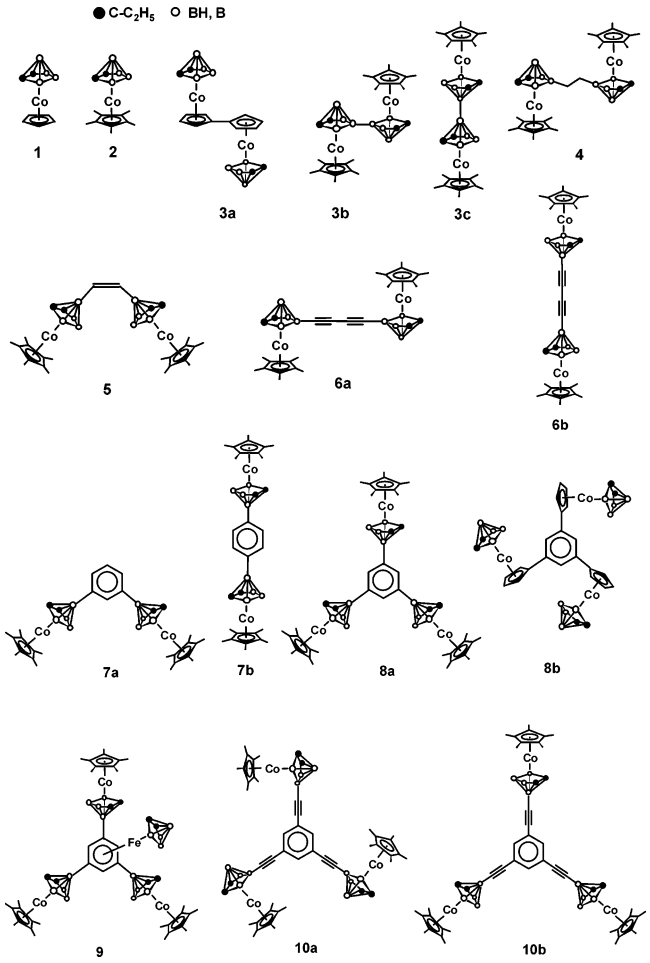

Chart 2

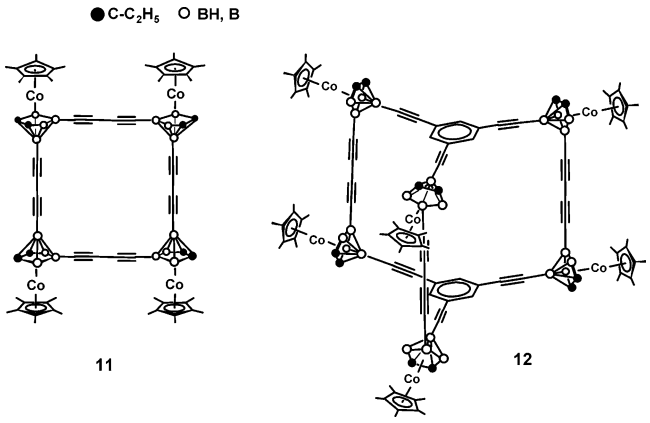

of cluster connectivity, allow us to study subtle electronic effects that govern the interactions between two cobaltacarborane subunits. Let us start with complexes **3a**−**c** whose clusters are directly linked with no intervening units. It was previously shown that the fulvalene-bridged complex **3a** exhibits two separate one-electron oxidations (in CH_2Cl_2) as well as two separate one-electron reductions (in thf),[8] where the separation of the two oxidations ($\Delta E^\circ = 0.25$ V) is slightly lower than that detected in biferrocene ($\Delta E^\circ = 0.35$ V).[9] The electrochemical and spectroelectrochemical features suggest that $\mathbf{3a}^+$ and $\mathbf{3a}^-$ are mixed-valent systems possessing partially and completely delocalized charges, respectively.[8]

Chart 3

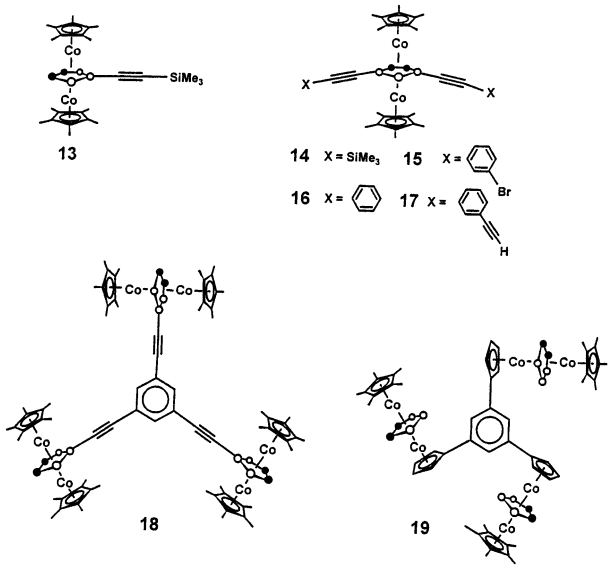

In the present study, cyclic voltammetry of the B−B connected dimer **3b** in CH_2Cl_2 solution shows a single oxidation coupled to chemical complications, in that the current ratio i_{pc}/i_{pa} at scan rates increasing from 0.02 V s^{-1} to 0.5 V s^{-1} remains below 1.0 (the highest ratio of 0.8 is reached at the highest scan rate). In addition, the current function $i_{pa} \cdot v^{-1/2}$ progressively decreases with increasing scan rate, eventually leveling off at a constant value which is about 2/3 of that observed at the lowest scan rate. Attempts to determine the number of electrons involved in the process via controlled potential coulometry were unsuccessful. However, given the similarity of the cyclic voltammetric pattern in **3b** to that of the analogous isoelectronic ferracarborane dimer [wherein (η^6-C_6H_6)Fe^{II} replaces Cp*Co^{III}], which involved a two-electron process in exhaustive electrolysis,[3a] it is very likely that the present process involves a primary oxidation to the monocation $\mathbf{3b}^+$, which in turn converts to a further oxidizable byproduct. This would imply that the expected second oxidation $\mathbf{3b}^{+/2+}$ is masked by the solvent discharge; in tetrahydrofuran solution the same oxidation pattern is maintained, but the lifetime of $\mathbf{3b}^+$ is even shorter. Unexpectedly, no reduction process was detected.

The apically linked dimer **3c** shows a first oxidation that is roughly similar to that of its equatorially linked isomer **3b**; in addition, **3c** exhibits a second oxidation, albeit an irreversible one. In contrast to **3b**, a one-electron reduction is found for **3c** in tetrahydrofuran solution. The redox potentials for these compounds are compiled in Table 1, together with those of other dinuclear species discussed below.

A few observations can be made concerning the directly linked dicobaltacarboranes **3a**-**3c**. (i) Connection through the

(8) (a) Chin, T. T.; Grimes, R. N.; Geiger, W. E. *Inorg. Chem.* **1999**, *38*, 93. (b) Chin, T. T.; Lovelace, S. R.; Geiger, W. E.; Davis, C. M.; Grimes, R. N. *J. Am. Chem. Soc.* **1994**, *116*, 9359.

(9) For data on biferrocene measured in CH_2Cl_2 solutions, see: (a) LeVanda, C.; Bechgaard, K.; Cowan, D. O. *J. Org. Chem.* **1976**, *41*, 2700. (b) LeVanda, C.; Bechgaard, K.; Cowan, D. O.; Rausch, M. D. *J. Am. Chem. Soc.* **1977**, *99*, 2964. (c) Kotz, J.; Neyhart, G.; Vining, W. J.; Rausch, M. D. *Organometallics* **1983**, *2*, 79. (d) Lee, M.-T.; Foxman, B. M.; Rosenblum, M. *Organometallics* **1985**, *4*, 539. (e) O'Connor Salazar, D. C.; Cowan, D. O. *J. Organomet. Chem.* **1991**, *408*, 227.

Table 1. Formal Electrode Potentials (V, vs SCE) and Peak-to-Peak Separations (mV; measured at 0.2 V s^{-1}) (in brackets) for the Redox Processes Exhibited by the Dinuclear Complexes

complex	$E^{\circ\prime}_{2+/+}$	$E^{\circ\prime}_{+/0}$	$E^{\circ\prime}_{0/-}$	$E^{\circ\prime}_{1-/2-}$	solvent
1[a]		+1.55			CH_2Cl_2
			−1.71		thf
2		+1.16 (*100*)			CH_2Cl_2
		+1.43 [b,c]	−1.99 (*88*)[b]		DME
3a[a]			−1.53	−1.99	thf
	+1.75	+1.50			CH_2Cl_2
3b		+0.85[c]			thf
		+0.61 (80)[d]			CH_2Cl_2
3c		+1.14 (100)	−2.15 (130)[d]		thf
	+1.36[c,e]	+1.00 (130)			CH_2Cl_2
4	+1.04[c,f]	+1.04[c,f]	−1.72 (*90*)[d,f]	−1.72 (*90*)[d,f]	CH_2Cl_2
5	+1.08[c]	+0.91[c]			CH_2Cl_2
6a	+1.50[c,e]	+1.18[c,e]	−1.69[e]	−1.74[e]	thf
	+1.48[c,e]	+1.15 (*100*)[d]	−1.77 (*50*)	−1.83 (*70*)	CH_2Cl_2
6b	+1.45[e]	+1.37[c,e]	−1.82 (*120*)	−1.94 (*120*)	thf
7a	+1.14[g,h]	+1.06[g,h]			CH_2Cl_2
7b	+1.15[g,h]	+1.07[g,h]			CH_2Cl_2
FcH		+0.53 (95)			thf
		+0.39 (70)			CH_2Cl_2

[a] From refs 8a,b. [b] From ref 10. [c] Peak-potential value for irreversible processes. [d] Partially chemically reversible. [e] Value estimated by differential pulse voltammetry. [f] Two-electron process. [g] Partially resolved one-electron processes. [h] From deconvolution voltammetry.

equatorial B(5) atoms strongly destabilizes the HOMO, resulting in a first oxidation that is ca. 0.5 V easier in **3b** than in its mononuclear precursor **2**; a similar effect was seen for the analogous iron dimer with respect to the corresponding monomer (η^6-C_6H_6)Fe($Et_2C_2B_4H_4$).[3a] (ii) A more attenuated cathodic shift is observed in isomer **3c**, in which the intercluster connection occurs through the apical B(7) atoms; the oxidation process is about 0.2 V more facile in **3c** than in the monomer **2**. (iii) If one assumes that a second oxidation of complex **3b** occurs at potential values higher than 1.5 V (i.e., beyond the anodic window of the solvent), then the relative separation of the two one-electron processes in complexes **3a**, **3b**, and **3c** suggests that B(5)−B(5) linkage allows stronger electronic interaction between the redox centers in the mixed-valent Co^{II}—Co^{III} monocation, than does B(7)−B(7) or Cp−Cp interconnection. Unfortunately, nothing can be concluded about the possible interaction between the redox centers in the mixed-valent monoanions, since the expected sequence of reduction steps is completely masked in **3b** and is only partially detected in **3c**.

Complex **4**, in which the B(5) vertexes are connected by a CH_2CH_2 bridge (a typical spacer which prevents effective electronic communication between two redox centers, as in diferrocenylethane)[11] displays a single, irreversible two-electron oxidation. Exhaustive oxidation of **4** generates the parent monomer $\mathbf{2}^+$, as revealed by the ultimate appearance of the corresponding reversible redox system. A single two-electron reduction of **4** with features of partial chemical reversibility is also observed. Complex **5** has a —CH=CH— linkage, which usually permits some electron conduction (as in diferrocenylethene,[11] for example), exhibits two slightly separated one-electron oxidations, which are irreversible in character. No reduction processes were detected. In view of the small 0.17 V separation of the two oxidation processes, it is likely that the elusive $\mathbf{5}^+$ belongs to the partially delocalized Robin-Day Class II.

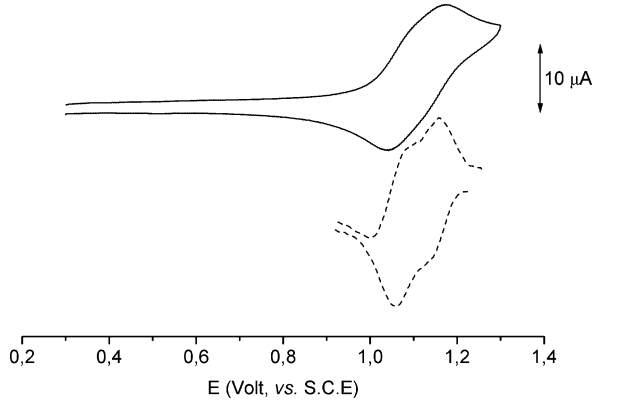

Figure 1. Cyclic (—) and deconvolution (- − -) voltammetric responses recorded at a platinum electrode in CH_2Cl_2 solution of **7a** (5×10^{-4} mol dm^{-3}). $[NBu_4][PF_6]$ (0.2 mol dm^{-3}) supporting electrolyte. (—) Scan rate 0.2 V s^{-1}.

The redox behavior of the diethynyl-linked isomers **6a** and **6b** has been described.[1] It is uncertain whether **6a** undergoes a single two-electron oxidation (complicated by subsequent chemical reactions) or two separate one-electron oxidations, the second of which takes place beyond the solvent discharge. Two nearly overlapping, partially chemically reversible one-electron reductions are observed. Considering just the cathodic process, the transient mixed-valent monoanion $\mathbf{6a}^-$ should be assigned to the localized Robin-Day Class I. We note that the (η^6-C_6H_6)-Fe^{II} analogue of **6a** displays a single two-electron oxidation, coupled to chemical complications,[3a] whereas 1,4-diferrocenyl-1,3-butadiyne undergoes two slightly separated one-electron oxidations ($\Delta E^\circ = 0.1$ V).[9a,12]

The electron-transfer properties of **6b** resemble those of **6a**, but the separation between the two reduction processes in **6b** is slightly higher ($\Delta E^\circ = 0.12$ V vs 0.05 V), suggesting that $\mathbf{6b}^-$ belongs to the partially delocalized Robin-Day Class II; in this case, unlike the directly B−B linked dimers **3b** and **3c**, electron delocalization is evidently greater in the apically vs the equatorially connected isomer.

Consider now the benzene-linked isomers **7a** and **7b**. These complexes exhibit nearly identical behavior, shown in Figure 1 for **7a**. Cyclic voltammetry of both compounds is consistent with a single two-electron oxidation possessing features of chemical reversibility. Both square wave and differential pulse voltammetric profiles show the occurrence of partially overlapping processes. The plot of the semi-derivative currents from cyclic voltammetry (deconvolution voltammetry)[13] allows us definitively to distinguish two peaks separated by 0.08 V. As confirmation that inter-cluster communication is slightly less in B−B connected dicobaltaboranes compared to their diferrocene analogues, we note that both *p*-phenylene-bridged and *m*-phenylene bridged diferrocenes undergo two slightly better-separated one-electron oxidations ($\Delta E^\circ = 0.10$ V, +0.09 V, respectively).[14]

(10) Stephan, M.; Hauss, J.; Zenneck, V.; Siebert, W.; Grimes, R. N. *Inorg. Chem.* **1994**, *33*, 4211.
(11) Ferguson, G.; Glidewell, C.; Opromolla, G.; Zakaria, C. M.; Zanello, P. *J. Organomet. Chem.* **1996**, *517*, 183.
(12) Adams, R. D.; Qu, B.; Smith M. D.; Albright, T. A. *Organometallics* **2002**, *21*, 2970.
(13) (a) Philp, R. H.; Reger, D. L.; Bond, A. M. *Organometallics* **1989**, *8*, 1714. (b) Oldham, K. B.; Philp, R. H. *Current Separations* **1990**, *10*, 3.
(14) Patoux, C.; Coudret, C.; Launay, J.-P.; Joachim, C.; Gourdon, A. *Inorg. Chem.* **1997**, *36*, 5037.

Table 2. Formal Electrode Potentials (V, vs SCE) and Peak-to-Peak Separations (mV; measured at 0.2 V s^{-1}) (in brackets) for the Redox Processes Exhibited by the Trinuclear Complexes

complex	$E^{o\prime}_{4+/3+}$	$E^{o\prime}_{3+/2+}$	$E^{o\prime}_{2+/+}$	$E^{o\prime}_{+/0}$	$E^{o\prime}_{0/-}$	$E^{o\prime}_{-/2-}$	$E^{o\prime}_{2-/3-}$	solvent
8a		+1.19[a]	+1.13[a]	+1.06[a]				CH_2Cl_2
8b		+1.45[b,c]	+1.45[b,c]	+1.45[b,c]	−1.53 (*60*)	−1.64 (*55*)	−1.76 (*50*)	thf
		+1.40[b,c]	+1.40[b,c]	+1.40[b,c]	−1.60 (*90*)	−1.71 (*90*)	−1.85 (*90*)	CH_2Cl_2
9	+1.74 [b,c]	+1.52[b,c]	+1.33[b,c]	+0.70 [d]	−1.92 (*60*)	−2.06 (*60*)	−2.16 (*60*)	thf
10a		+1.34[b,c]	+1.34[b,c]	+1.34[b,c]	−1.80(*100*)	−1.80 (*100*)	−1.80 (*100*)	thf
		+1.15 (*80*)[e]	+1.15 (*80*)[e]	+1.05 (*80*)[e]				CH_2Cl_2
10b		+1.36[b,c]	+1.36[b,c]	+1.36[b,c]	−1.95 (*95*)	−2.10 (*95*)	−2.20 (*95*)	thf
		+1.32 (*70*)[f]	+1.20 (*70*)[f]	+1.04 (*70*)[f]				CH_2Cl_2

[a] From deconvolution voltammetry. [b] Peak-potential value for irreversible processes. [c] From differential pulse voltammetry. [d] Iron-centered process (see text). [e] Complicated by following chemical reactions. [f] $[NBu_4][B(C_6F_5)_4]$ supporting electrolyte.

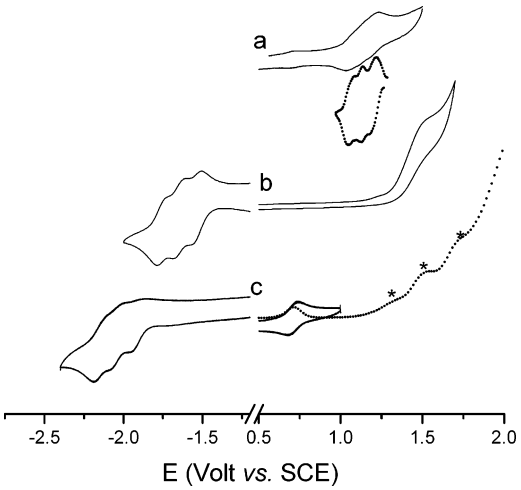

Figure 2. Cyclic (—) and deconvolution (- − -) voltammetric responses recorded at a platinum electrode in CH_2Cl_2 solution of (a) **8a** (1×10^{-4} mol dm^{-3}) and (b) **8b** (3×10^{-4} mol dm^{-3}). (**c**) Cyclic (—) and Osteryoung square wave (•••) voltammetric responses recorded at a gold electrode in thf solution of **9** (2×10^{-4} mol dm^{-3}). $[NBu_4][PF_6]$ (0.2 mol dm^{-3}) supporting electrolyte. Scan rates 0.2 V s^{-1}.

Although the overall oxidation processes of **7a** and **7b** exhibit features of chemical reversibility on the cyclic voltammetry time scale, the original yellow solutions turn green upon exhaustive electrolysis ($E_w = +1.2$ V) but the original voltammetric profiles disappear, indicating that the corresponding cations are not indefinitely stable. No reduction steps were found within the cathodic window (up to −2.2 V).

Trinuclear Cobaltacarboranes. The cyclic voltammetric profile of the benzene-centered species **8a**, shown in Figure 2a, is reminiscent of that of the related dinuclear complex **7a**. Cyclic voltammetry shows an apparent single, chemically reversible three-electron oxidation; however, by means of deconvolution voltammetry the overall oxidation is resolved into three separate processes ($\Delta E^\circ \approx 0.06$ V). No reduction step was detected up to −2.2 V.

Coordination of a fourth metallacarborane unit to the benzene ring, as in the heterotetranuclear $FeCo_3$ complex **9**, affords four observable oxidations (Figure 2c). The first, chemically reversible, step may reasonably be assigned to the $Fe^{II}-Fe^{III}$ couple, whereas the further cobalt-centered oxidation processes are partially covered by the solvent discharge, making it difficult to determine their chemical reversibility. Controlled potential coulometry of the first oxidation ($E_w = +0.8$ V) consumes one electron per molecule, and the resulting solution exhibits a cyclic voltammetric profile quite complementary to the original one, demonstrating the long-term chemical stability of $\mathbf{9}^+$. Complex **9** also undergoes three separate reduction processes.

While detection of the cobalt-centered oxidation steps is ambiguous, these are clearly anodically shifted in **9** with respect to **8a**. Conversely, the iron-centered oxidation process is cathodically shifted (by about 0.3 V) relative to $(\eta^6\text{-}C_6H_6)Fe(Et_2C_2B_4H_4)$,[3a] indicating a significant transfer of electron density from the cobaltacarborane units to the central ferracarborane unit. Complex **8b** shows an irreversible three-electron oxidation and three separate reversible reductions (Figure 2b); it was not possible in this case to resolve the overall oxidation. The pertinent formal electrode potentials are compiled in Table 2, together with those of the remaining tricobaltacarboranes. With respect to complexes **8a** and **8b**, it seems likely that permethylation of the cyclopentadienyl ring in **8a** is the main source of the anodic shift of both the oxidation and the reduction processes relative to the nonmethylated complex **8b**.

The redox behavior of the triethynylbenzene-linked complexes[1] **10a** and **10b** is interesting. In dichloromethane solution, **10b** displays a reversible three-electron oxidation, which in the presence of the weakly coordinating supporting electrolyte[15] $[NBu_4][B(C_6F_5)_4]$ splits into three close one-electron oxidations. Three close reductions are also observed in tetrahydrofuran solution. A similar pattern holds for **10a**, except that only a partial separation of the oxidation peaks in two subsequent processes is seen, even when $[NBu_4][B(C_6F_5)_4]$ is present. In this connection, we have previously pointed out[1] that the contrast between this behavior and that of tris(ferrocenylethynyl)benzene, which exhibits a single three-electron oxidation, is evidence of significant intramolecular interaction in the tricobaltacarboranes.

Tetranuclear and Hexanuclear Cobaltacarboranes. As communicated earlier,[2a] cyclic voltammetry on the planar octagonal tetramer **11** (Chart 2) reveals two well-separated one-electron reductions followed by a single two-electron reduction, indicating measurable intramolecular electronic communication between the four cobalt centers. The simultaneous entry of the last two electrons is likely due to the fact that, following the first stepwise two-electron addition, the two remaining Co(III) centers become energetically equivalent. In turn, the oxidation path appears to involve, in sequence, a one-electron removal followed by a second multielectron oxidation, both processes being irreversible.[2a] It is interesting to compare the redox potentials of such redox changes with those of the dimers **6a** and **6b** (Table 3), both of which can be regarded as building blocks of the tetramer. These data are consistent with a view of **11** as a bis(diethynyl)-linked dimer of either two **6a** or two **6b** moieties, and do not particularly favor one over the other.

The macrocyclic hexamer **12**[6g] (Chart 2) may be viewed either as a trimer of 6a units connected by tris(ethynyl)benzene spacers,

(15) LeSuer, R. J.; Geiger, W. *Angew. Chem. Int. Ed.* **2000**, *39*, 248

Table 3. Comparison between the Formal Electrode Potentials (V, vs SCE) for the Redox Processes Exhibited by Complexes 11 and 12 and Their Low-Nuclearity Counterparts, in thf Solution [Peak-to-Peak Separations (mV; measured at 0.2 V s^{-1}) in Brackets]

complex	$E^{\circ\prime}_{\text{second ox}}$	$E^{\circ\prime}_{\text{first ox}}$	$E^{\circ\prime}_{\text{first red}}$	$E^{\circ\prime}_{\text{second red}}$	$E^{\circ\prime}_{\text{third re}}$
11	+1.45[a,b,c]	+1.26[a,b,d]	−1.55 (*60*)[d]	−1.65 (*60*)[d]	−1.84 (*80*)[e]
6a	+1.50[a,b]	+1.18[a,b]	−1.69[a,d]	−1.74[a,d]	
6b	+1.45[a,b]	+1.37[a,b]	−1.82 (*120*)	−1.94 (*120*)	
12	+1.5[a,b,c]	+1.16[a,b,c]	−1.62 (60)[c]	−1.75 (60)[c]	
10b		+1.36[a,c]	−1.95 (*100*)	−2.10 (*100*)	−2.20 (*100*)

[a] Peak-potential values for irreversible processes. [b] From differential pulse voltammetry. [c] Three-electron process. [d] One-electron process. [e] Two-electron process. [f] Partially chemically reversible.

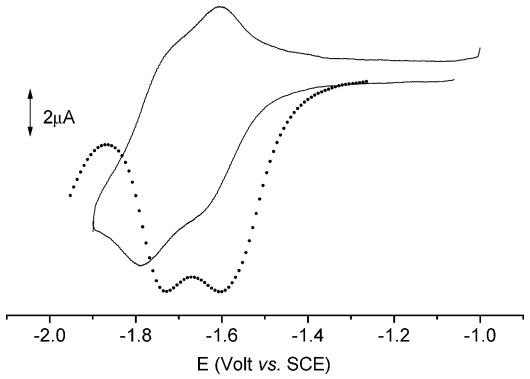

Figure 3. Cyclic (—) and differential pulse (···) voltammetric responses recorded at a gold electrode in a thf solution of **12** (1.3×10^{-4} mol dm^{-3}). $[NBu_4][PF_6]$ (0.2 mol dm^{-3}) supporting electrolyte. Scan rates: (—) 0.2 V s^{-1}; (···) 0.02 V s^{-1}.

or alternatively as a dimer of **10b** modules linked by three butadiyne chains. As illustrated in Figure 3, its cyclic voltammogram displays two separated, chemically reversible, reductions at potential values very close to those observed for 6a (Table 3) as well as two irreversible oxidations not shown in the figure. These findings suggest that the intramolecular electronic communication essentially arises from the coupling of cobalt centers within each **6a**-type moiety, whereas the triethynyl-benzene linkages connecting these units have almost no effect.

On this basis, we can reasonably assume that each reduction (as well as oxidation) process involves the simultaneous exchange of three electrons. Compared to the behavior of **6a**, the chemical reversibility of both reduction processes in **12** is markedly improved. A plausible interpretation of this finding is that any destabilization that is produced on addition of electron density to **12** is mitigated by the multiple connections present in this large system.

Triple-Decker Cobaltacarboranes. As previously reported,[1] the B(5)-trimethylsilylethynyl complex **13** (Chart 3) undergoes two well-separated oxidations and reductions (only the first step of each couple is chemically reversible on the cyclic voltammetric time scale), which highlight the ability of the central C_2B_3 ring to allow strong electronic interaction between the two face-bonded cobalt centers. The same is true in the related B(4,6)-diethynyl complexes **14**−**17** (Chart 3). Consequently, both the mixed-valent monocations and monoanions of the triple-decker complexes clearly belong to the fully delocalized Robin-Day Class III. It is notable that the redox potentials of all the processes of complexes **15**−**17**, which are compiled in Table 4, clearly show a positive linear relation with the inductive effect of the substituents at the phenyl ring, as evaluated by the Taft parameter F.[16]

Reflecting the fact that for distant substituents field effects are dominant over resonance effects, it was not possible to obtain any reasonable fit with the resonance Taft parameter R. Interestingly, the inductive role played by the substituents becomes more important on subsequent electron additions to the different dications; thus the slope of the linear best fit increases from 0.13 for **15**−**17**$^{2+/+}$ to 0.66 for **15**−**17**$^{-/2-}$.

Controlled potential coulometry corresponding to the first anodic process for complexes **13**−**17** shows the consumption of one electron per molecule, during which the original red-orange solutions turn red-brown. Cyclic voltammetry on the resulting solutions indicates that the electrogenerated cations **14**$^+$, **16**$^+$, and **17**$^+$ are stable also on the bulk electrolysis time scale, while **13**$^+$ and **15**$^+$ undergo minor decomposition.

The redox behavior[1] of the "triple-triple-decker" complex tris-[B(5)-ethynylcobaltacarborane]benzene (**18**, Chart 3) is similar to that of the corresponding triple-decker monomer CpCo(2,3-$C_2B_3H_5$)CoCp,[17] undergoing two well-separated oxidation and reduction processes. The first oxidation and first reduction are both chemically reversible on the time scale of cyclic voltammetry, while the second oxidation and reduction are chemically irreversible. Controlled potential coulometric measurement of the first oxidation indicates the consumption of three electrons per molecule and causes a color change from orange to brown.

Table 4. Formal Electrode Potentials (V, vs SCE) for the Redox Processes Exhibited by the Triple-Decker Complexes [Peak-to-Peak Separations (mV; measured at 0.2 V s^{-1}) in Brackets]

complex	$E^{\circ\prime}_{\text{second ox}}$	$E^{\circ\prime}_{\text{first ox}}$	$E^{\circ\prime}_{\text{first red}}$	$E^{\circ\prime}_{\text{second red}}$	$E^{\circ\prime}_{\text{third red}}$	$E^{\circ\prime}_{\text{fourth red}}$	solvent
13		+0.36 (*80*)[a]	−1.81 (*70*)[a]	−2.80[a,b,c]			thf
	+1.38[a,b,c,]	+0.12 (*100*)[a]					CH_2Cl_2
14	+1.36[a,b,c]	+0.33 (*70*)[a]	−1.76 (*70*)[a]	−2.71[a,b,c]			thf
	+1.27[a,b,c]	+0.10 (*85*)[a]	−1.90[a,c]				CH_2Cl_2
15	+1.42[a,b,c]	+0.44 (*60*)[a]	−1.62 (*120*)[a]	−2.40[a,b,c]			thf
	+1.30[a,b,c]	+0.17 (*70*)[a]	−1.82[a,c]				CH_2Cl_2
16	+1.36[a,b,e]	+0.35 (*100*)[a]	−1.73 (*60*) [a]	−2.70[a,b,e]			thf
	+1.24[a,b,e]	+0.11 (*70*)[a]	−1.87[a,e]				CH_2Cl_2
17	+1.39[a,b,c]	+0.39 (*95*)[a]	−1.72 (*100*)[a]	−2.53[a,b,c]			thf
	+1.30[a,b,c]	+0.17 (*110*)[a]	−1.85[a,c]	−			CH_2Cl_2
18		+0.32 (*120*) [d]	−1.82 (*70*)[d]	−2.80[b,e,d]			thf
	+1.40[b,c,d]	+0.17 (*230*)[d,e]					CH_2Cl_2
19	+1.40[b,c,d]	+0.42 (*80*)[d]	−1.70 (*60*)[a]	−1.75 (*60*)[a]	−1.82 (*60*)[a]	−2.7[b,c,d]	thf
	+1.35[b,c,d]	+0.27[b,c,d,e]	−1.80[a,b,c]	−1.86[a,b,c]	−1.92[a,b,c]		CH_2Cl_2

[a] One-electron process. [b] Peak-potential values for irreversible processes. [c] From differential pulse voltammetry. [d] Three-electron process. [e] Three partially resolved one-electron processes.

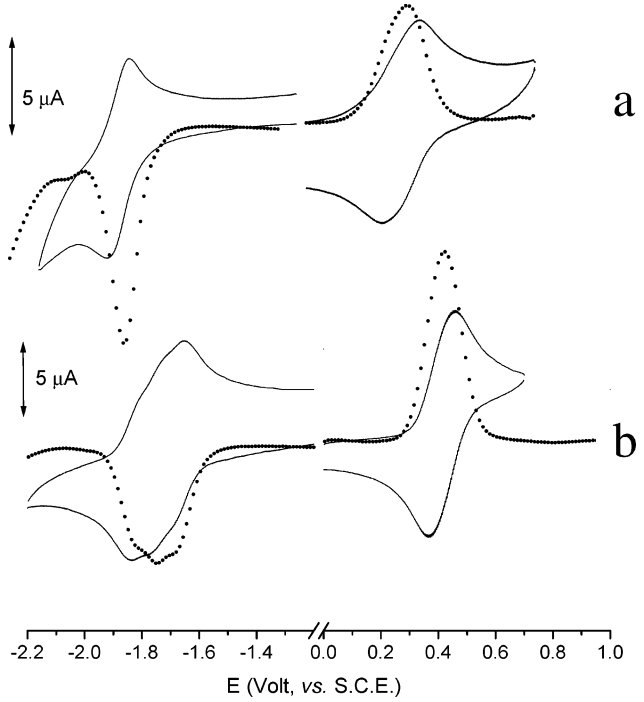

Figure 4. Cyclic (—) and differential pulse (···) voltammetric responses recorded at a gold electrode in thf solutions of (a) **18** (4.0×10^{-4} mol dm^{-3}) and (b) **19** (2.6×10^{-4} mol dm^{-3}). $[NBu_4][PF_6]$ (0.2 mol dm^{-3}) supporting electrolyte. Scan rates: (—) 0.2 V s^{-1}; (···) 0.02 V s^{-1}.

Cyclic voltammetric tests after exhaustive oxidation indicate that the electrogenerated trication $\mathbf{18}^{3+}$ undergoes partial decomposition.

A similar overall redox pattern is observed for the related pinwheel complex **19**, in which the triple-decker units are linked to the central benzene ring via cyclopentadienyl ligands. However, Figure 4 reveals an interesting difference in the cyclic voltammetric behavior of **18** and **19**. In **18**, the first oxidation generates a broad profile, whereas that of the first reduction is much narrower; the opposite is seen for **19**. In the latter case, the signal of the first oxidation is quite narrow, whereas the signal of the first reduction is broad enough to be resolved into three successive, closely spaced processes. Such small separations are normally taken to indicate the absence of extensive electronic delocalization between the redox centers, and this assumption has been confirmed by spectroelectrochemistry. Furthermore, as we discuss below, the nature of the orbitals involved in these redox processes supports the presence of a weak intramolecular electronic communication. As shown in Table 4, substitution of one of the two pentamethylcyclopentadienyl rings in each triple-decker moiety (in **18**) by an unsubstituted cyclopentadienyl ligand (in **19**) induces an anodic shift by about 0.1 V for each of the redox processes.

Spectroelectrochemistry. Despite the general lability of electrogenerated species in macroelectrolysis experiments, spectroelectrochemical analysis in an OTTLE cell allowed us to define the nature of the mixed-valent species involved in the electron transfer processes of a few representative families. Our efforts were directed mainly to a search for intervalence transition (IT) bands that give further insight into the classification of mixed-valent species based on cyclic voltammetry. As

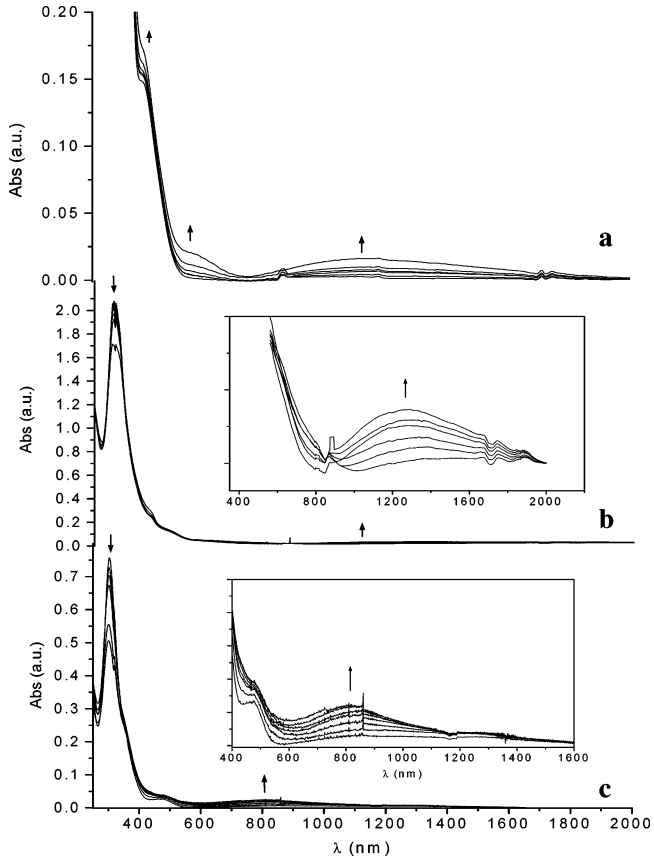

Figure 5. UV−vis−NIR spectra of (a) **6b**, (b) **11**, and (c) **12**, showing changes on reduction. Thf solutions containing $[NBu_4][PF_6]$ (0.2 mol dm^{-3}) as supporting electrolyte. Spectra were stepwise recorded in an OTTLE cell after each interval of 2 min of applied potential ($E_w = -1.80$ V for **6b**, −1.55 V for **11**; −1.60 V for **12**).

a general criterion, spectra were collected up to the disappearance of the isosbestic points, a feature which has been assumed as diagnostic for decomposition of electrogenerated species. Given the fact that the addition or removal of electrons is often followed by decomposition, measurement of molar absorptions is pointless since precise concentrations of the different species are not known; for this reason, spectral absorptions are expressed in arbitrary units. As direct comparisons of the intensity of the IT bands are precluded, quantitative estimates of the coupling interactions are not possible. The spectral changes induced by reduction of **6b** are illustrated in Figure 5a.

With the addition of one electron, two new bands appear; the same behavior is displayed by complex **6a**. In both cases, the lower energy absorption has a bandwidth at half-height that is slightly larger than the theoretical value expected for class II IT bands: $\Delta\nu_{1/2} = 48\sqrt{\bar{\nu}}$, where $\Delta\nu_{1/2}$ is the half-height bandwidth and $\bar{\nu}$ is the wavenumber (in cm^{-1}).[18] For $\mathbf{6a}^-$: $\Delta\nu_{1/2\ (IT,\ theoretical)} = 4460\ cm^{-1}$ vs $\Delta\nu_{1/2\ (experimental)} = 4720\ cm^{-1}$; for $\mathbf{6b}^-$: $\Delta\nu_{1/2\ (IT,\ theoretical)} = 4800\ cm^{-1}$ vs $\Delta\nu_{1/2\ (experimental)} = 5030\ cm^{-1}$. These results strongly support the presence of an IT process, and suggest that both $\mathbf{6a}^-$ and $\mathbf{6b}^-$ should be classified as partially delocalized class II mixed-valent species. These findings are consistent with the electrochemical behavior of **6b** described above, but are in partial disagreement with that of **6a**. Since the monoanions decomposed after a few scans, the

(16) Hansch, C.; Leo, A.; Taft, R. W. *Chem. Rev.* **1991**, *91*, 165.
(17) Brennan, D. E.; Geiger, W. E., Jr. *J. Am. Chem. Soc.* **1979**, *101*, 3399.
(18) Hush, N. S. *Prog. Inorg. Chem.* **1967**, *8*, 391.

Table 5. Electronic Spectral Data for Complexes **6a-b**, **11**, **12**, **13**, **18**, **19**, and Their Electrogenerated Species [OTTLE Cell, thf /$[NBu_4][PF_6]$ (0.2 mol dm^{-3}) Solution. ↑ Increasing during Electrolysis; ↓ Decreasing during Electrolysis]

complex	λ (nm)
6a	343, 460
$\mathbf{6a}^-$	343, 460↑, 605, 1160
6b	315, 345, 408
$\mathbf{6b}^-$	315, 345, 408↑, 600, 1130
11	316, 475
$\mathbf{11}^-$	316↓, 475, 1250
12	304, 350, 480
$\mathbf{12}^{3-}$	304↓, 350↓, 480, 810
13	308, 355, 427, 516, 751
$\mathbf{13}^+$	280↑, 355↓, 405, 548, 751↓, 912, 1050
$\mathbf{13}^-$	308↑, 355↓, 427↓, 516↑, 751↓, 1040
18	353, 437, 510, 753
$\mathbf{18}^+$	353↓, 397, 545, 655, 753↓, 880, 1070
19	355, 410, 520, 780
$\mathbf{19}^-$	355↓, 520↑, 780↓, 1005

expected disappearance of the IT bands in the dianions $\mathbf{6a}^{2-}$ and $\mathbf{6b}^{2-}$ could not be observed.

Reductions of the tetranuclear complex **11** (Figure 5b) and the hexanuclear complex **12** (Figure 5c) afforded qualitatively similar results; in the case of $\mathbf{11}^-$ the half-height bandwidth is only slightly larger than the theoretical value: $\Delta\nu_{1/2(\text{IT, theoretical})} = 4270\ cm^{-1}$ vs $\Delta\nu_{1/2(\text{experimental})} = 4400\ cm^{-1}$, whereas for $\mathbf{12}^{3-}$ the observed bandwidth is somewhat larger than the theoretical: $\Delta\nu_{1/2\ (\text{IT, theoretical})} = 5440\ cm^{-1}$ vs $\Delta\nu_{1/2\ (\text{experimental})} = 7890\ cm^{-1}$. On this basis, $\mathbf{11}^-$ and $\mathbf{12}^{3-}$ can be definitely described as class II mixed-valent complexes. As in other cases, the reduced species decompose and all the bands diminish in intensity, so that further spectral evolution upon generating $\mathbf{11}^{2-}$ or $\mathbf{12}^{6-}$ was not observable. All of the spectral data pertinent to these complexes are compiled in Table 5.

We turn now to the triple-decker sandwiches. Geiger et al.[19] carried out spectroelectrochemical measurements on the one-electron oxidation of $(p\text{-}MeC_6H_4CHMe_2)_2Ru_2(Et_2C_2B_3H_3)$, which exhibits an electrochemical behavior resembling that of the present complexes **13**−**17**. It was found that the electrogenerated monocation $[(p\text{-}MeC_6H_4CHMe_2)_2Ru_2(Et_2C_2B_3H_3)]^+$ can be described as completely delocalized mixed-valent class III. In support of this conclusion, none of the bands exhibited a bandwidth as large as that required for a class II mixed-valent complex, and the solvent independence of the absorptions was not consistent with an IT band assignment.[19] In the present study, spectroelectrochemical experiments on both the oxidation and reduction of complex **13** (Figures 6a and 7a) led to similar conclusions about this system. While detailed assignment of the spectra of $\mathbf{13}^+$, **13**, and $\mathbf{13}^-$ is not straightforward (primarily owing to the presence of many weak low energy absorptions), their narrowness rules out the possibility that such bands might be ascribed to IT processes.

Spectroelectrochemical measurements were also carried out on **18** and **19** and the respective spectra were compared with that of the parent complex **13**. Since the electrochemical behavior foreshadowed the possible formation of mixed-valent species along the oxidation path of **18** and the reduction path of **19**, we studied such a spectroelectrochemical evolution, looking for the possible evidence of electronic interaction. As

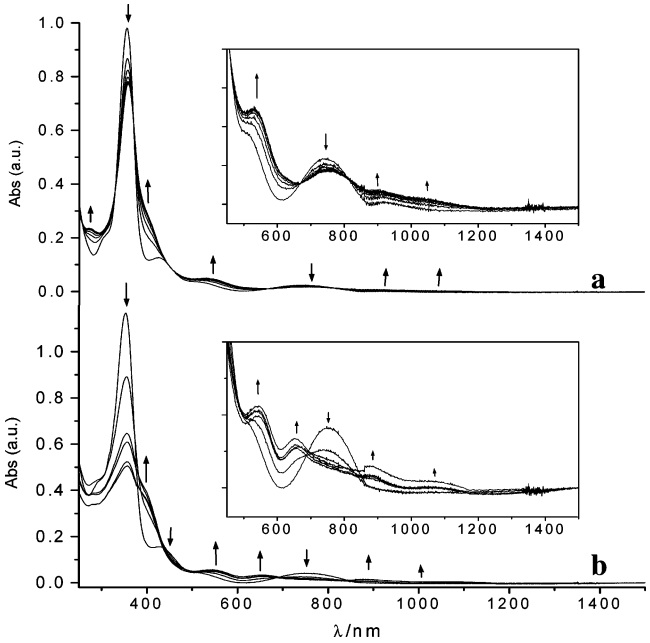

Figure 6. UV−vis−NIR spectra of (a) **13** and (b) **18** showing changes on oxidation, in thf solutions containing $[NBu_4][PF_6]$ (0.2 mol dm^{-3}) as supporting electrolyte. Spectra were stepwise recorded in an OTTLE cell after each interval of 2 min of applied potential (E_w = +0.35V for **13**; +0.30 V for **18**).

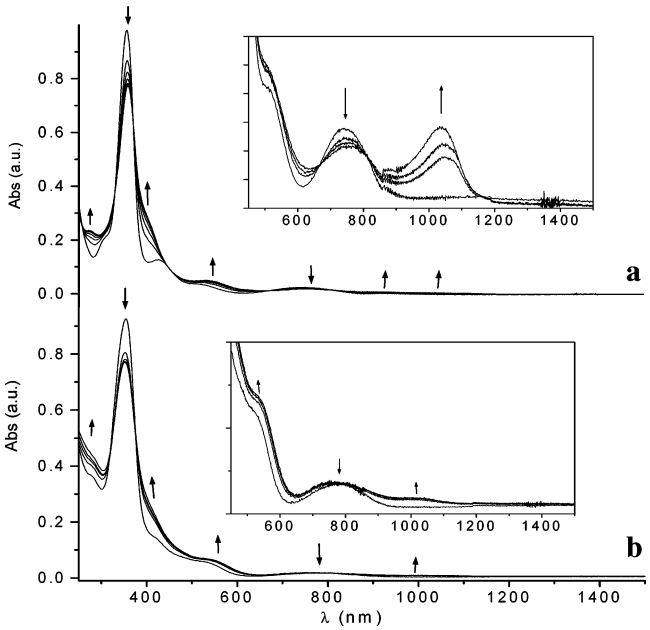

Figure 7. UV−vis−NIR spectra of (a) **13** and (b) **19** showing changes on reduction, in thf solutions containing $[NBu_4][PF_6]$ (0.2 mol dm^{-3}) as supporting electrolyte. Spectra were stepwise recorded in an OTTLE cell after each interval of 2 min of applied potential (E_w = −1.80V for **13**; −1.70 V for **19**).

shown in Figure 6b, the spectrum recorded upon oxidation of **18** is very similar to that of $\mathbf{13}^+$, apart from a further new band at 655 nm, which is also too narrow to be a reliable candidate as an IT band. Analogously, the spectrum recorded upon reduction of **19** (Figure 7b) is very similar to that of $\mathbf{13}^-$. On the basis of these observations, in agreement with the cyclic voltammetric results, we conclude that there is no reliable evidence for intramolecular electronic communication *between* the triple-decker subunits in **18** and **19**.

(19) Merkert, J. W.; Davis, J. H., Jr.; Geiger, W. E.; Grimes, R. N. *J. Am. Chem. Soc.* **1992**, *114*, 9846.

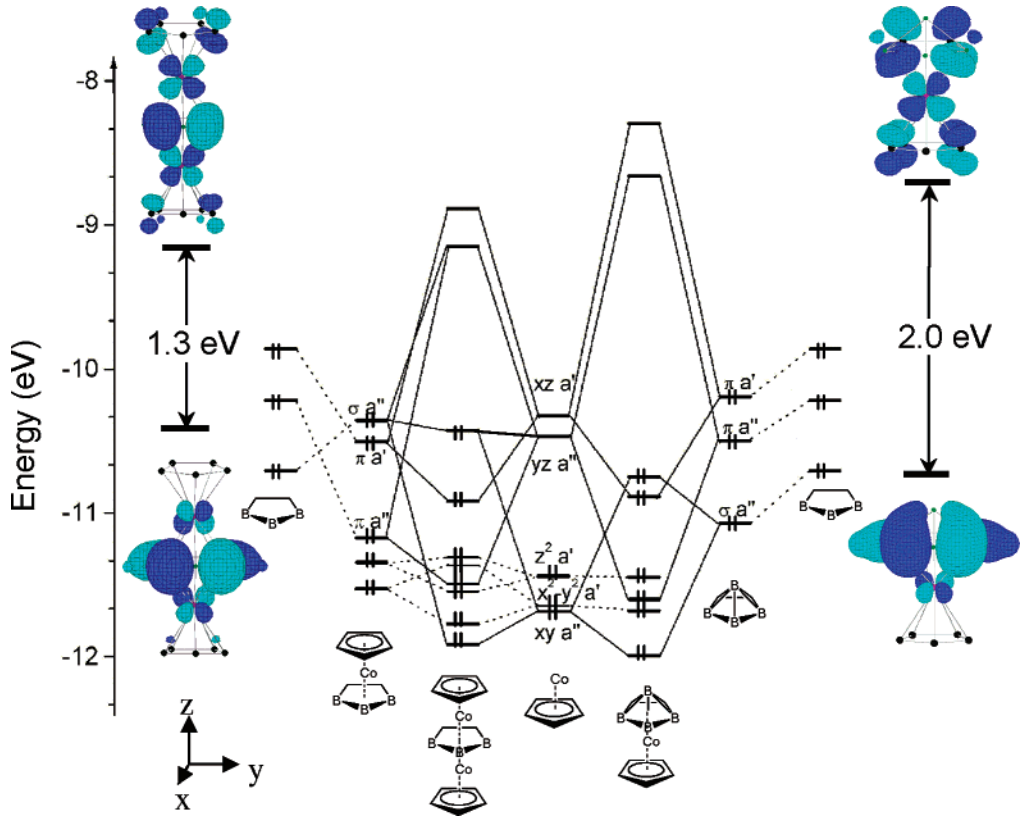

Figure 8. Interaction between the frontier orbitals of the apical BH^{2+} and $CpCo^{2+}$ fragments with the $C_2B_3H_5^{4-}$ ring (right and left side) to form $C_2B_4H_6^{2-}$ and $C_2B_3H_5CoCp^{2-}$, respectively. The interaction between the frontier orbitals of $C_2B_4H_6^{2-}$ or $C_2B_3H_5CoCp^{2-}$ with $CpCo^{2+}$ (center) to form the sandwich complex $CpCoC_2B_4H_6$ and the triple-decker complex $CpCoC_2B_3H_5CoCp$ is depicted in the middle of the diagram. The reference system and the fragments are shown at the bottom. Hydrogen atoms are omitted for clarity.

Molecular Orbital Calculations. An extended Hückel study was conducted in order to gain insight into the redox behavior of the cobaltacarboranes. Fragment analyses were performed for two model complexes, consisting of a triple-decker and a double-decker sandwich unit, respectively. These models and fragments thereof, together with the reference system, are shown at the bottom of Figure 8. The figure depicts the interaction between the orbitals of $CpCo^{2+}$ (shown at center) and those of the $C_2B_4H_6^{2-}$ and $CpCoC_2B_3H_5^{2-}$ fragments to generate the $CpCoC_2B_4H_6$ double-decker and $CpCoC_2B_3H_5CoCp$ triple-decker sandwiches, respectively.

The changes accompanying the interaction between the apical BH^{2+} or $CpCo^{2+}$ units with the $C_2B_3H_5^{4-}$ ring are depicted at the right and left side of the diagram, respectively. The symmetry labels used are those of the C_s point group, which is the lower symmetry exhibited by the models or fragments discussed here and is imposed by the $CpCoC_2B_4H_6$ model. Filled π and σ orbitals of the $C_2B_3H_5^{4-}$ ring are involved in the relevant bonding in these model complexes, all of them stabilized by interaction with the apical BH^{2+} fragment (Figure 8, right). On the opposite side, when the $C_2B_3H_5^{4-}$ orbitals interact with the apical $CpCo^{2+}$ fragment the σ orbital is destabilized while the two π MOs are stabilized (Figure 8, left).

For both the triple-decker and double-decker sandwich models, the HOMO and LUMO have a'' symmetry: these are the combinations of the π a″ and σ orbitals of $C_2B_4H_6^{2-}$ or $CpCoC_2B_3H_5^{2-}$ with the d_{xy} and d_{yz} orbitals of the $CpCo^{2+}$ fragment. In the case of the sandwich complex $CpCoC_2B_4H_6$, the low lying, filled d_{xy} orbital of $CpCo^{2+}$ and the σ orbital of $C_2B_4H_6^{2-}$ adequately match in energy, as do the high lying, empty d_{yz} and π a'' orbitals. In this case, the mixing is unimportant and the HOMO is the antibonding combination of the d_{xy} and σ orbitals, while the LUMO is the antibonding combination of the d_{yz} and π a'' orbitals.

In contrast, in the triple-decker $CpCoC_2B_3H_5CoCp$ system the order of the σ and π a'' orbitals of $CpCoC_2B_3H_5^{2-}$ fragment is reversed, as is the match in energy between the corresponding orbitals. As a consequence of this, and also because of the better overlap between d_{yz} and both σ and π, orbital mixing is important. Therefore, the HOMO, which can still be described as the antibonding combination of d_{xy} of $CpCo^{2+}$ and the σ orbital of the $CpCoC_2B_3H_5^{2-}$ fragment, has a nonnegligible contribution from the d_{yz} orbital of the $CpCo^{2+}$, and is destabilized with respect to the HOMO of $CpCoC_2B_4H_6$.

Analogously, the LUMO is the antibonding combination of the d_{yz} and π a″ orbitals, but has a nonnegligible contribution from the σ orbital and is stabilized with respect to the LUMO of the $CpCoC_2B_4H_6$ cluster. This may explain the large cathodic shift upon oxidation, as well as the anodic shift of the reduction, in the triple-decker family relative to that of the $CpCoC_2B_4H_6$ double-decker sandwiches. Moreover, even the LUMO+1 of the triple-decker is lower in energy than the LUMO of the $CpCoC_2B_4H_6$ unit, while the HOMO-1 of the triple-decker is close in energy to the HOMO of $CpCoC_2B_4H_6$, suggesting that these orbitals may be involved in the second electron addition/removal. In any case, owing to the energy match between the orbitals of the fragments, covalence is approached so that both the HOMO and LUMO of these models have strong contributions from both the cobalt atoms and the carborane ligand. Consequently, while assignment of formal oxidation states to

the cobalt atoms is useful for comparative purposes, the actual charge distribution within the clusters is much less sharply defined than these imply.

Notwithstanding the qualitative basis of the semiempirical approach, closer examination of the frontier orbitals of the triple-decker sandwich throws light on a possible explanation of the redox behavior observed for **18** and **19**, discussed above (see Figure 4). Since the HOMO of the triple-decker has no contribution from the Cp rings, it is reasonable to think that three corresponding, unperturbed, orbitals will be present in **19**, in which three triple-decker units are connected via their Cp ligands. As a result, the three-electron oxidation of **19** occurs in one step. The LUMO of the triple-decker, on the other hand, has a significant contribution from the Cp rings, and the pathway for electronic communication between redox centers is open; this is consistent with an energy spread among the three corresponding orbitals present in **19**. The reverse is true for **18**, in which three triple-decker units are connected via the central C_2B_3 ring, which is a major contributor to the HOMO of the triple-decker model but is less so to the LUMO.

Conclusions

This study is part of a cooperative program in which designed syntheses of extended polynuclear systems are conducted in parallel with detailed probes of electronic structure and properties. Ultimately, the goal is to develop the synthetic methodology and electronic understanding to a point allowing true exploitation of this chemistry for practical purposes.[20] The current investigation of cobaltacarborane systems, building on previous electrochemical studies involving carborane complexes of iron, ruthenium, cobalt, and other metals,[1−3,7,8,10,17,19] allows some generalizations that should help to guide future work in this area.

Of central interest, of course, is the question of metal−metal communication and its influence by a variety of factors, including the nature and oxidation state of the metal(s), the metallacarborane clusters selected as building-block units, the selection of linking groups between clusters, the position of attachment of the linkers on the cluster skeletons, the identity and location of attached substituents, and, for extended two- and three-dimensional assemblies, their macro architecture.[20] As this and earlier work demonstrates, the effects of these variables on electronic structure and properties are complex, often subtle, and at this stage only partially understood, but some trends are emerging and we summarize these here.

Thus far, based on electrochemical and more selective spectroelectrochemical investigations, full electron delocalization (Robin-Day class III) has been observed in two types of small metallacarborane systems:

- Cations or anions generated via oxidation or reduction of multidecker sandwiches containing planar $C_2B_3H_5^{4-}$ rings (or substituted derivatives), as in compounds **13**−**19** in the present study and earlier examples,[3b] and the ruthenium triple-deckers $[(p\text{-}MeC_6H_4CHMe_2)_2Ru_2(Et_2C_2B_3H_3)]$;[19]
- Dicobalt fulvalene-bridged complexes of type **3a**[8] and oligomeric chains of tetradecker sandwich stacks constructed from **3a**-type units.[21]

In the multidecker complexes, extended Hückel calculations show that the very strong overlap between the carborane ligand HOMO and the metal d orbitals is the principal factor in the delocalization.

In *directly linked* $CpCoC_2B_4$ Co^{II}−Co^{III} mixed-valent clusters, metal−metal communication is strongly dependent upon the mode of connection, i.e., between apex boron atoms, equatorial boron atoms, or via Cp−Cp bonding, as illustrated in the series **3a**−**3c**. As discussed above, direct linkage between equatorial boron atoms [B(5)−B(5)] leads to greater metal−metal interaction than does apex-to-apex [B(7)−B(7)] bonding, reflecting larger destabilization of the HOMO (relative to the parent monomer) in the equatorial-linked vs the apical-linked systems. The same effect was observed previously in analogous Fe^{II}−Fe^{III} iron-arene dimers.[3a]

Biscobaltacarborane complexes in which the cluster units are separated by intervening groups (**4**, **5**, **6a**, **6b**) exhibit localized or partially delocalized redox behavior. Not surprisingly, the dimethylene-linked **4** is Robin-Day Class I (fully localized), while the ethenyl-connected complex **5** shows partial delocalization (Class II). In the case of the diethynyl-bridged isomers **6a** and **6b**, electrochemical measurements imply that their anions exhibit different behavior: the equatorially linked **6a**$^-$ shows no delocalization and is assigned to Class I, while the apically connected **6b**$^-$ is Class II. However, spectroelectrochemical analysis establishes that both **6a**$^-$ and **6b**$^-$ are partially delocalized Class II systems. In this case, unlike the directly linked dimers **3b** and **3c**, delocalization is favored by apical rather than equatorial substitution.

Metal−metal communication in phenylene-bridged bis- and triscobaltacarboranes is generally difficult to detect via cyclic voltammetry but is observable via square wave or differential pulse voltammetry. The weak intercage communication in biscobaltacarboranes **7a** and **7b** is slightly less than that seen in phenylene-bridged diferrocenes, but it is increased substantially when thiophene is interposed as a linker between FeC_2B_4 clusters.[3a] In the tricobaltacarboranes **8a,b** and **10a,b** the limited metal−metal communication is higher than in tris(ferrocenylethynyl)benzene, the analogue of **10a**, where mutual interaction is completely absent.

Measurable delocalization is also present in macrocycles having four to six cobaltcarboranes connected via −C≡C−C≡C− chains. Here, the effects of macromolecular architecture begin to be seen as well. As discussed above, comparison of the redox properties of the octagonal-planar tetramer **11** with the dimers **6a** and **6b** shows that **11** can be viewed as an assembly of either **6a** or **6b** modules. In contrast, the hexamer **12** is clearly a trimer of **6a** units, i.e., electron delocalization occurs mostly within the individual CoC_2B_4−C≡C−C≡C−C_2B_4Co moieties rather than across the triethynylbenzene connectors. Spectroelectrochemical studies conclusively demonstrate that **11**$^-$ and **12**$^{3-}$ are partially delocalized mixed-valent systems.

In the tris(triple-decker) phenylene-bridged complexes **18** and **19**, detailed spectroelectrochemical analysis shows that, as in all MC_2B_3M triple-deckers studied to date, there is full delocalization *within* the sandwich units, but no clear evidence of communication between them.

(20) (a) Grimes, R. N. *Pure Appl. Chem.* **2003**, *75*, 1211. (b) Grimes, R. N., In *Contemporary Boron Chemistry*; Davidson, M., Hughes, A. K., Marder, T. B., Wade, K., Eds.; Royal Society of Chemistry: London, 2000, 283−290. (c) Grimes, R. N. *Molecular Crystals and Liquid Crystals* **2000**, *342*, 7−14.

(21) (a) Meng, X.; Sabat, M.; Grimes, R. N. *J. Am. Chem. Soc.* **1993**, *115*, 6143. (b) Geiger, W. E., private communication.

Taken together, the current state of the art in synthesis, combined with electronic findings in this and earlier studies, suggest that nanoscale devices employing small metallacarborane building-block units with specified architectures and having electronic components (insulators, semiconductors, and conductors) in desired locations, are possible in principle. The attractive features of these compounds — their general robustness in redox processes, adaptability to many different metals, metal oxidation states, and substitution chemistry, solubility in organic solvents, and utility in constructing a wide array of geometrically novel macrostructures — should, in time, overcome the disadvantage of their more difficult accessibility compared to conventional organometallics. Advances in small borane and carborane synthesis utilizing readily available bulk chemical starting materials such as boric acid[22] and $NaBH_4$[23] suggest that this time may be not too distant.

Experimental Section

Anhydrous 99.9% dichloromethane was an Aldrich product. Anhydrous 99.9%, HPLC grade tetrahydrofuran (Aldrich) was distilled in the presence of sodium before use. Fluka $[NBu_4][PF_6]$ (electrochemical grade) was used as supporting electrolyte (0.2 mol dm^{-3}). Cyclic voltammetry was performed in a three-electrode cell containing a platinum working electrode surrounded by a platinum-spiral counter electrode, and an aqueous saturated calomel reference electrode (SCE) mounted with a Luggin capillary. A BAS 100W electrochemical analyzer was used as polarizing unit. All the potential values are referred to the saturated calomel electrode (SCE). Under the present experimental conditions, the one-electron oxidation of ferrocene occurs at $E^{\circ\prime} = +0.39$ V and $E^{\circ\prime} = +0.53$ V in dichloromethane and in tetrahydrofuran solutions, respectively. Controlled potential coulometry was performed in an H-shaped cell with anodic and cathodic compartments separated by a sintered-glass disk. The working macroelectrode was a platinum gauze; a mercury pool was used as the counter electrode. The UV−vis spectroelectrochemical measurements were carried out using a Perkin-Elmer Lambda 900 UV−vis spectrophotometer and an OTTLE (optically transparent thin-layer electrode) cell[24] equipped with a Pt-minigrid working electrode (32 wires/cm), Pt minigrid auxiliary electrode, Ag wire pseudoreference and CaF_2 windows. The electrode potential was controlled during electrolysis by an Amel potentiostat 2059 equipped with an Amel function generator 568. Nitrogen-saturated solutions of the compound under study were used with $[NBu_4][PF_6]$ (0.2 mol dm^{-3}) as supporting electrolyte. Working potential was kept fixed at the peak potential of the process under study and spectra were progressively collected after each 2 min electrolysis.

Extended Hückel calculations were performed using the CACAO98 for windows programs package.[25] Bond distances and angles of the model molecule were taken as the average of the experimental values. Slater orbital ionization energies have been corrected from the default ones by taking H_{ii} from a set of values calculated from DFT theory.[26] The exponentials of the Slater orbitals were taken from the program library.

Acknowledgment. P. Z. gratefully acknowledges financial support from the University of Siena (PAR 2003). The syntheses and characterizations were supported by National Science Foundation Grant No. CHE 9980708 to R. N. G. We thank J. Monte Russell for the synthesis of **4**.

Supporting Information Available: Experimental data on the synthesis and spectroscopic characterization of **4**, **7a**, and **14**−**17** (7 pages, print/PDF). This material in PDF format is available free of charge via the Internet at http://pubs.acs.org.

JA047966L

(22) Adams, L.; Hosmane, S. N.; Eklund, J. E.; Wang, J.; Hosmane, N. S. *J. Am. Chem. Soc.* **2002**, *124*, 7292.
(23) (a) Ryschkewitsch, G. E.; Miller, V. R. *J. Am. Chem. Soc.* **1975**, *97*, 6258. (b) Miller, V. R.; Ryschkewitsch, G. E. *Inorg. Chem.* **1974**, *15*, 118. (c) Hosmane, N. S.; Grimes, R. N. *Inorg. Chem.* **1979**, *18*, 3294.
(24) Krejčik, M.; Daněk, M.; F. Hartl, F. *J. Electroanal. Chem.* **1991**, *317*, 179.
(25) Mealli, C.; Proserpio, D. M. *J. Chem. Educ.* **1990**, *67*, 390.
(26) Vela, A.; Gázquez, J. L. *J. Phys. Chem.* **1988**, *92*, 5688.